buildings

MDPI

Article

Research on Arrangement of Measuring Points for Modal Identification of Spatial Grid Structures

Chunjuan Zhou [1,2], Jinzhi Wu [1], Guojun Sun [1,*], Jie Hu [1], Qize Xu [1], Yang Li [1] and Mingliang Liu [2]

[1] College of Architectural and Civil Engineering, Beijing University of Technology, Beijing 100124, China; harvestzhou@163.com (C.Z.); kongjian@bjut.edu.cn (J.W.); hujie0403@163.com (J.H.); xuqize5316@163.com (Q.X.); 13848465181@163.com (Y.L.)

[2] Shaanxi Architecture Science Research Institute Co., Ltd., Xi'an 710082, China; liumingliang-35@163.com

* Correspondence: sunguojun@bjut.edu.cn

Abstract: In structural health monitoring, because the number of sensors used is far lower than the number of degrees of freedom of the structure being monitored, the optimization problem of the location and number of sensors in the structures is becoming more and more prominent. However, spatial grid structures are complex and diverse, and their dynamic characteristics are complex. It is difficult to accurately measure their vibration information. Therefore, an appropriate optimization method must be used to determine the optimal positioning of sensor placement. Aiming at the problem that spatial grid structures have many degrees of freedom and the fact that it is difficult to obtain complete vibration information, this paper analyzed the typical EI method, MKE method, and EI-MKE method in the arrangement of the measuring points, and it was verified that the EI method was more suitable for the vibration detection of spatial grid structures through the example of a plane truss and spatial grid structures. Measuring points under the assumption of structural damage were explored, and it was proposed that there might have been a stable number of measuring points that could cover the possible vibration mode changes in the structures. At the same time, combined with the three-level improved Guyan recursive technique, in order to obtain better complete modal parameters, the influence of the number of measuring points on the complete vibration mode information was studied. It was concluded that MAC_d was better than MAC_n as the quantitative target.

Keywords: spatial grid structures; layout of measuring points; vibration mode expansion; modal identification

Citation: Zhou, C.; Wu, J.; Sun, G.; Hu, J.; Xu, Q.; Li, Y.; Liu, M. Research on Arrangement of Measuring Points for Modal Identification of Spatial Grid Structures. *Buildings* **2024**, *14*, 2338. https://doi.org/10.3390/buildings14082338

Academic Editor: Nuno Mendes

Received: 26 June 2024
Revised: 20 July 2024
Accepted: 23 July 2024
Published: 28 July 2024

1. Introduction

As a kind of large-span structures, spatial grid structures have the characteristics of a complex form and a huge volume. It is impossible and unnecessary to obtain the response data of the structures through a large number of sensors [1–3]. The early optimal arrangement of sensors was based on the establishment of the finite element model of the structures and the arrangement of sensors based on experience. This method is more practical, but it can only be used for structures with fewer degrees of freedom. In the optimization of the number and location of sensors for complex and multi-node structures, it is very difficult to optimize the number and location of sensors only by experience, which makes it difficult to meet the requirements. Therefore, it is of great significance for the effective operation of whole-health monitoring systems to study and determine the optimal arrangement positions and reasonable number of sensors.

The optimal placement of sensors first needs to determine the objective function, and the principle is to obtain as much structural information as possible. One class of methods aims at the linear independence of the target mode [4,5]. For example, Kammer [6] proposed the effective independence method (EI) in 1991. The basic idea of the algorithm is to construct an idempotent matrix so that the measured points are linearly independent

and orthogonal to each other as much as possible. Lim [7], combined with the eigensystem realization method, carried out sensor placement with the minimum condition number of the Hankel matrix. Wu et al. [8] proposed a sensor placement method based on a two-step method from the two aspects of the number and location of the sensors. Bao [9] studied the optimal placement of sensors for arched roofs and trussed roofs. Based on the EI method, the optimal placement criteria or general rules of the sensors are given. The other method of determining the objective function is to consider the arrangement of the measuring points from the perspective of energy. The modal kinetic energy method [10] (MKE) is used to arrange the measuring points with the maximum kinetic energy of the target mode. Gomes [11] determined the optimal sensor placement of dynamic systems from the perspective of parameter identification based on Fisher's information matrix from the perspective of obtaining structural information. In addition, the MinMAC method aims to minimize the maximum element value of the off-diagonal element of the modal assurance criterion matrix to select the sensor position in order to maximize the angle between the measured modal shape vectors. Considering the advantages and disadvantages of the EI method and the MKE method, Liu et al. [12] proposed an improved optimal sensor placement method, namely, the effective independence–modal kinetic energy method (EI-MKE). Li Dongsheng et al. [13] deeply analyzed the relationship between the MKE method, EI method, MinMAC method, modal matrix method, and other methods, and they revealed their differences and connections. The example showed that there were no two methods to determine the sensor position that were exactly the same. Zhang et al. [14] proposed a data-driven OSP strategy that achieves structural damage detection based on vibration sensors by precisely reconstructing modal shapes using only a few sensors that are incorporated into an SHM system. Zhan et al. [15] determined the optimal (and worst) locations for AE source localization in sensor clusters with unknown material properties of isotropic plates through a Bayesian optimal sensor placement strategy. Xu et al. [16] utilized convolutional neural networks for an ensemble-based data assimilation optimal sensor placement method. Guo et al. [17] proposed a new performance-based sensor optimization configuration method based on the proposed indicators of modal observability and damage detectability and introduced an OSP method for a single-line radar.

Damage identification is an important part of structural health monitoring [18,19]. In practical engineering, due to the limitation of the number of sensors and the measurement conditions, only limited measuring points can be monitored to obtain incomplete low-order vibration modes [20–23]. Some scholars have studied the application of model order expansion in damage identification. Xiao Feng et al. [24] studied a damage identification stiffness separation method for large spatial truss structures based on static response. Xiao Feng et al. [25] proposed a damage identification method for slender beam frame structures. Liu et al. [26] proposed a direct expansion method for mode expansion by using a composite vector composed of the measured value of the main degree of freedom and the estimated value of the slave degree of freedom, and they used the MAC method to evaluate the expansion results. Brincker et al. [27] used the SEREP method to expand the vibration mode of the plate numerical model after smoothing the measured vibration mode. These methods achieve the expansion of modal shapes by solving the transfer matrix and rely too much on the finite element analysis mode rather than the actual engineering state. Zhao et al. [28] used the SEREP method to expand the mode shape, established a linear system of equations for the damage coefficient, and used the Moore–Penrose generalized inverse to solve the equations. On the basis of the dynamic condensation method, Mousavi et al. [29] iteratively modified the damage coefficient and the model condensation matrix using only the translational degrees of freedom of the first mode of vibration for damage identification, but they still needed to measure more degrees of freedom. Aiming at the problem of limited measuring points and test noise in damage identification, Yang et al. [30] used a parametric dynamic condensation method to expand the vibration mode. Civalek et al. [31] used the DSC-HDQ method to solve the geometric nonlinear dynamic problem of a rectangular plate on an elastic foundation.

Based on the above analysis, it can be seen that in the process of modal parameter identification of large-span spatial structures with complex shapes, numerous nodes, and dense frequency, on the basis of the difference between the actual state of the structures and the theoretical model, the location of the sensors, the number and order of the selected modes, and the number of layouts still need to be further studied. At the same time, the application of modal order expansion in spatial grid structures, especially how to effectively link it with the arrangement of the measuring points in its inverse process and check whether the arrangement of the measuring points in the structures is reasonable, is still rare. In this paper, aiming at the problem that spatial grid structures have many degrees of freedom and it is difficult to obtain complete vibration information, a method of measuring a point arrangement that is suitable for spatial grid structures is verified and analyzed by an example. Combined with the three-stage improved Guyan recursive technique, the influence of the number of measuring points on obtaining the complete vibration mode information is studied. The suggestion that the measuring point can be preset before the dynamic detection of the spatial grid structures is put forward.

2. Applicability Analysis of Measuring Point Arrangement Method

The traditional measuring point optimization algorithm is essentially a process of finding the optimal solution. According to the defined objective function, the iterative optimization is carried out by using the different matrices formed. As shown in Table 1, the different measuring point arrangement methods proposed by different scholars essentially change the objective function of the optimization process and then search in the solution domain according to different objective functions. The search order is divided into three processes: gradual deletion, direct acquisition, and gradual accumulation. The suboptimal solution found by iteration is close to the optimal solution, which can usually meet the requirements of measuring point arrangement.

Table 1. The objective function of different measuring point arrangement methods.

Measuring Point Arrangement Method	Effective Independence Method (EI)	Modal Assurance Criterion (MAC)	Modal Kinetic Energy (MKE)	Covariance Matrix (VM)
Objective function	The estimation of the model coordinate estimation error covariance is the smallest.	The maximum element of the non-diagonal element of the MAC matrix is the smallest.	The kinetic energy of the modal degree of freedom is the largest.	The linear unbiased estimation error of the modal matrix is the smallest.
Target	The contribution to the target mode is the largest.	The spatial intersection angle of the modal vector of the measuring point is the largest.	The signal-to-noise ratio is the maximum	The ability to obtain the vibration mode and the signal strength are the largest.

The above measuring point algorithm has been widely used in engineering [32,33]. From the existing research, the contribution of the measuring point to the mode and the energy of the measuring point are the two factors that have the greatest influence on the structure; the EI method can efficiently select the degree of freedom that contributes a lot to the target mode shape; the MKE method improves the signal-to-noise ratio of the measuring point with the goal of degree-of-freedom energy. Therefore, this paper chooses the EI, MKE, and EI-MKE methods, three representative methods, to study the applicability of measuring point arrangement in spatial grid structures.

2.1. Principle of Measuring Point Arrangement Method

2.1.1. Effective Independence Method (EI) [34,35]

The EI method constructs the effective independence matrix E by solving the characteristic equation of Fisher's information matrix:

$$E = \Phi\left(\Phi^T\Phi\right)^{-1}\Phi^T \tag{1}$$

In the Equation (1), E is an idempotent matrix, whose diagonal elements satisfy $0 \leq E_{ii} \leq 1$, and the ith element represents the contribution of the ith degree of freedom to the rank of matrix E. If E_{ii} is close to 0, the degree of freedom contributes less to the linear independence of the target mode and should be removed; if E_{ii} is close to 1, the degree of freedom contributes more to the linear independence of the target mode and should be retained.

The starting point of constructing matrices by the EI method is that the vectors used to construct them are orthogonal. If the constructed vectors are not orthogonal, the orthogonal and cross orthogonal tests used in the derivation of EI method will cause large errors. For the orthogonal vibration mode $\Phi = \Phi_x\ \Phi_y\ \Phi_z$, the orthogonal test should be conducted:

$$\beta = \left[\Phi_x\Phi_y\Phi_z\right]^T\left[\Phi_x\Phi_y\Phi_z\right] = \Phi_x\Phi_x + \Phi_y\Phi_y + \Phi_z\Phi_z \tag{2}$$

Because the vibration mode is orthogonal, that is, β= 0, and considering the spatial structure, it is impossible to satisfy the three directional components of the structural mode, that is, $\Phi_x\Phi_x = 0$, $\Phi_y\Phi_y = 0$, $\Phi_z\Phi_z = 0$.

Thus, E represents the effective independent distribution of the set of candidate sensor positions, and the elements on the diagonal of E represent the linearly independent contribution of the corresponding sensor candidate points to the modal matrix. After the matrix E is obtained, the priority order of each candidate point is sorted according to the diagonal element size after the matrix E is obtained. The iterative algorithm is used to eliminate the smallest measurement point of the corresponding diagonal element each time, and the next iteration is then carried out until the required number of measurement points is reached. Through this iterative algorithm, the linear independence of the modal matrix is preserved as much as possible, that is, the characteristics of the original structure are preserved.

2.1.2. Modal Assurance Criterion (MAC) [36]

The modal confidence factor MAC is a good tool to evaluate the intersection angle of modal vectors. It can reflect the correlation between two spatial vectors, and its calculation formula is as follows:

$$MAC_{ij} = \frac{\left({\Phi_i}^T\Phi_j\right)^2}{\left({\Phi_i}^T\Phi_j\right)\left({\Phi_i}^T\Phi_j\right)} \tag{3}$$

In the Equation (3), Φ_i and Φ_j are mode vectors of order i and j, respectively.

MAC_{ij} is located between 0 and 1, where 0 means that the two vectors are orthogonal, and 1 means that the two vectors are completely related. Therefore, the larger the non-diagonal elements of the MAC, the greater the correlation of the vectors, and the worse the independence of the modes of each order. The smaller the non-diagonal elements of the MAC, the better the independence of the modes of each order, and the better the characteristics of the original structure can be reflected. Generally, when the MAC is greater than 0.9, the two vectors are correlated, and the two vectors are indistinguishable. When it is less than 0.25, the two vectors are approximately considered orthogonal to each other.

2.1.3. Modal Kinetic Energy Method (MKE) [10]

The objective criterion of the MKE method is to find the set of measuring points so that the modal kinetic energy at the measuring points is the largest when the structure has the same number of measuring points. The modal kinetic energy expression is as follows:

$$MKE = \Phi^T M \Phi \tag{4}$$

In the Equation (4), M is the mass matrix obtained by the numerical modeling of the structure.

The contribution of the p-th degree of freedom to the kinetic energy of the q-th order mode is calculated as:

$$K_{pq} = \Phi_{pq} \sum_{s=1}^{n} M_{ps} \Phi_{sq} \tag{5}$$

The total contribution of the p-th degree of freedom to the kinetic energy of all target modes is given by:

$$K_p = \sum_{q=1}^{m} \Phi_{pq} \sum_{s=1}^{n} M_{ps} \Phi_{sq} \tag{6}$$

In the Equation (6), Φ_{pq} is the PTH element of the QTH mode; M_{ps} is the PTH row and s-th column element of the mass matrix M; and Φ_{sq} is the s-th element of the QTH mode. The optimum test point is determined based on the degree of freedom that contributes the most to the kinetic energy of a certain mode or the average kinetic energy of the target mode.

2.1.4. Covariance Matrix (VM) [37–39]

The covariance matrix method is based on the maximum information subset technique, which is used to solve the sensor optimization problem. Let matrix $Y = \{Y_s Y_p\} = [\Phi]^T$ be the modal matrix composed of the modal vectors of all feasible measuring points, and assume matrix $Y = \{Y_s Y_p\} = [\Phi]^T$, where Y_s is the modal mode of s observed measuring points, and Y_p is the modal mode of p unobserved measuring points, when Y_s is used to estimate Y_p linearly and without bias:

$$\hat{Y_p} = C_{pp} C_{ss}^{-1} Y_s \tag{7}$$

Among them, C_{ss} and C_{pp} are the diagonal submatrices of the matrix covariance matrix.

$$|cov(Y)| = \begin{vmatrix} C_{ss} & C_{sp} \\ C_{ps} & C_{pp} \end{vmatrix} = \begin{vmatrix} cov(Y_s) & C_{sp} \\ C_{ps} & cov(Y_p) \end{vmatrix} = |C_{ss}||D_{pp}| \tag{8}$$

where d is the estimated error

$$D_{pp} = cov\hat{Y_p}(-Y_p) = C_{pp} - C_{ps} C_{ss}^{-1} C_{sp} \tag{9}$$

Minimizing D_{pp} ensures an unbiased estimate of the mode displacement for unobserved measurement points using s sensors. As can be seen from Equation (9), this is equivalent to maximizing C_{ss}, that is, maximizing $|cov(Y_s)|$.

2.1.5. Effective Independence–Modal Kinetic Energy Method (EI-MKE)

EI-MKE method corrects EI method directly by multiplying the modal kinetic energy vector with the effective independent vector.

The EI method is directly revised by multiplying the modal kinetic energy vectors by the effective independent vectors.

$$EI_{MKE} = diag\left(\Phi\left(\Phi^T\Phi\right)^{-1}\Phi^T\right) \cdot diag\left(\Phi^T \Phi M\right) \tag{10}$$

2.2. Evaluation Criteria of Measuring Point Arrangement Results

Commonly used evaluations of test results include the energy, MAC, and determinant of Fisher's information matrix. This paper also evaluates the advantages and disadvantages of these three measuring point arrangement methods based on the energy angle, the orthogonality of the modal vector, and the determinant value of the Fisher information matrix. Due to the characteristics of the spatial bar structure, the extraction of the structural stiffness matrix and the mass matrix becomes easy to realize. Therefore, this paper proposes to improve the Guyan recursive technique and the complete modal MAC matrix of the theoretical modal expansion of the measuring point to evaluate the measurement point arrangement results.

2.2.1. Energy

The higher the energy of the candidate measuring points, the higher the signal-to-noise ratio that can be obtained in the test process, which is conducive to obtaining accurate structural parameters. The modal kinetic energy of the candidate measuring points is used to evaluate the arrangement of measuring points. The calculation of its value is the same as in Formula (3).

2.2.2. MAC

The MAC was originally proposed to detect structural damage and for damage location. It is now widely used in the correlation analysis of two curves. It is the most effective tool to judge the correlation between modes [1,2], especially test modes and theoretical modes.

$$MAC_{ij} = \frac{\left(\Phi_i{}^T \Phi_j\right)^2}{\left(\Phi_i{}^T \Phi_j\right)\left(\Phi_i{}^T \Phi_j\right)},\ j = 1, 2, 3, \ldots, m \tag{11}$$

According to Formula (4), the MAC matrix with the same number of output points is obtained. The diagonal elements represent the correlation between the two test curves, and the diagonal elements of the MAC matrix are represented by the MAC value. The higher the correlation between the two test curves, the closer the MAC value is to 1. The closer the MAC value of the two test curves is to 0, the more irrelevant the two test curves are. The MAC matrix of the feature vector formed by the candidate measuring points is used to evaluate the results of the measuring point arrangement. It is an index used to examine the advantages and disadvantages of the selected measuring points from the perspective of the linear independence of the modal vector. The smaller the off-diagonal element is, the larger the space vector intersection angle of the arranged measuring points.

2.2.3. The Determinant of Fisher's Information Matrix

$$F = lg\left(\frac{F_{select}}{F_{full}}\right) \tag{12}$$

According to the logarithm of the ratio of the determinant value of the Fisher information matrix at the selected measuring point position to the determinant value of the Fisher information matrix of the initial complete model, the information content of the selected measuring point containing the modal parameters is evaluated. The larger the F value, the more information about the structural modal parameters that is obtained.

2.2.4. Modal Expansion

The expansion process of the incomplete mode is based on the improved Guyan recursive technique. The principle is as follows:

The characteristic equation of an n-degree-of-freedom system is as follows:

$$Kx = \lambda Mx = f \tag{13}$$

According to the principal coordinate x_m and the vice coordinate x_s, the characteristic equation is divided into:

$$\begin{bmatrix} K_m & K_s \end{bmatrix} \begin{bmatrix} x_m \\ x_s \end{bmatrix} = \lambda \begin{bmatrix} M_m & M_s \end{bmatrix} \begin{bmatrix} x_m \\ x_s \end{bmatrix} \tag{14}$$

In the Equation (14), $K_m,\ M_m \in R^{N,m}$; $K_s,\ M_s \in R^{N,s}$, $m + s = N$

$$K_m = \begin{bmatrix} K_{mm} \\ K_{sm} \end{bmatrix},\ M_m = \begin{bmatrix} M_{mm} \\ M_{sm} \end{bmatrix},\ K_s = \begin{bmatrix} K_{ms} \\ K_{ss} \end{bmatrix},\ M_s = \begin{bmatrix} M_{ms} \\ M_{ss} \end{bmatrix} \tag{15}$$

Without considering the inertia force at the right end, the following is obtained:

$$\begin{bmatrix} K_m & K_s \end{bmatrix} \begin{bmatrix} x_m \\ x_s \end{bmatrix} = 0 \tag{16}$$

The coordinate transformation of the improved Guyan reduction is established from the above formula:

$$x_s = D_z x_m \tag{17}$$

$$D_z = -K_s^+ K_m \tag{18}$$

$$Ks+ = (KsTKs) - 1KsT \tag{19}$$

Furthermore, the improved Guyan in reduced form is obtained.

$$x = \begin{bmatrix} I \\ D_z \end{bmatrix} x_m = T_z x_m \tag{20}$$

$$K_z = T_z^T K T_z = K_{mm} + K_{ms} D_z + \mathrm{D}_z^T K_{sm} + \mathrm{D}_z^T K_{ss} D_z \tag{21}$$

$$M_z = T_z^T M T_z = M_{mm} + M_{ms} D_z + D_z^T M_{sm} + D_z^T M_{ss} D_z \tag{22}$$

Using the above improved Guyanreduced solution to approximate the right-side inertial force of Formula (7), the k-order reduced matrix of the improved Guyan is obtained:

$$D^{(k)} = D_z + K_s^+ (M_m + M_s D^{(k-1)}) [M^{(k-1)}]^{-1} K^{(k-1)} \tag{23}$$

$$K^{(k-1)} = K_{mm} + K_{ms} D^{(k-1)} + D^{(k-1)T} K_{sm} + D^{(k-1)T} K_{ss} \tag{24}$$

$$M^{(k-1)} = M_{mm} + M_{ms} D^{(k-1)} + D^{(k-1)T} M_{sm} + D^{(k-1)T} M_{ss} D^{(k-1)} \tag{25}$$

In the improved Guyan recursive technique, the retained principal coordinates are the degrees of freedom of the measuring points calculated by each measuring point algorithm. According to the obtained reduced matrix and the modes of the measuring points, the modal matrix of the whole structure is inversely deduced, and the MAC matrix of the calculated overall modal matrix and the theoretical modal matrix is calculated to evaluate the effectiveness of the measuring point arrangement. Practice shows that considering the calculation accuracy and calculation time, the three-stage improved Guyan recursive indentation technique can meet the requirements.

2.3. Research on Search Order of Algorithm

The plane truss structure shown in Figure 1 was established by using the finite element software Midas Gen 2024 v1.1. The chord length is 1.5 m, and the height is 1.2 m. The elastic modulus of the bar is 2.06×10^{11} N/m^2, the material density of the bar is 7.85×10^3 kg/m^3,

the cross-sectional area is 3.96×10^{-4} m^2, and the additional mass of the joint is 1050 kg. The first six natural frequencies and vibration modes of the structure were calculated as shown in Figure 2.

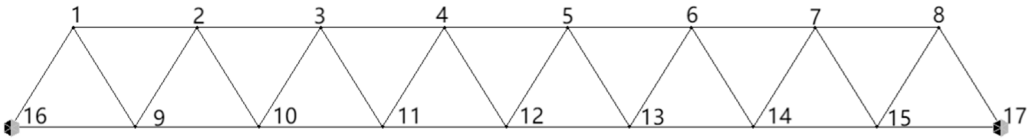

Figure 1. Midas Gen plane truss structure model.

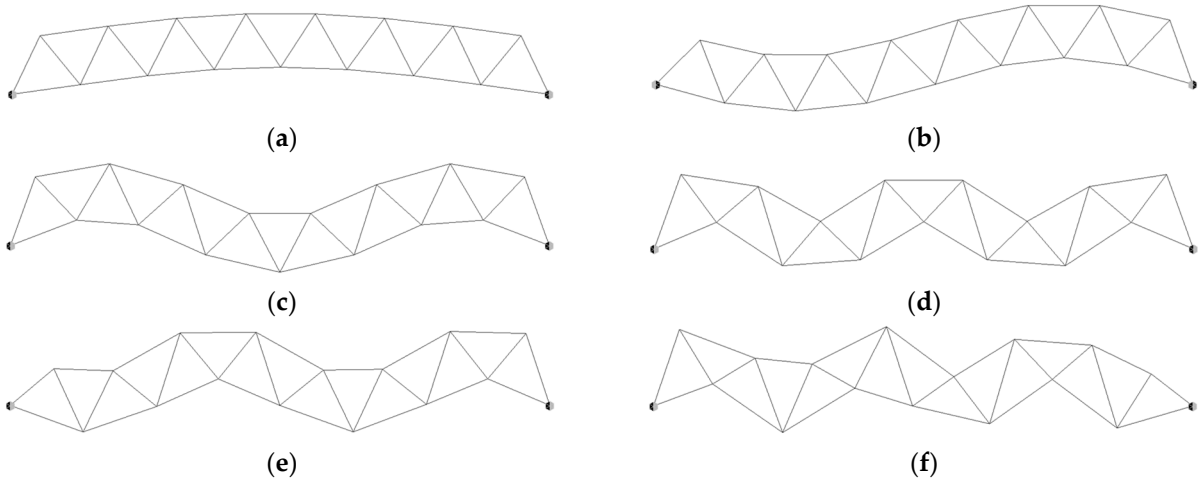

Figure 2. The first six modal frequencies and mode shapes of plane truss. (**a**) First mode of vibration (2.883 Hz); (**b**) Second-order vibration mode (6.981 Hz); (**c**) Third-order vibration mode (11.053 Hz); (**d**) Fourth-order vibration mode (13.386 Hz); (**e**) Fifth-order vibration mode (19.402 Hz); (**f**) Sixth-order vibration mode (21.025 Hz).

The targeting of the first six patterns and the selection of the six measuring points was achieved, and the layout schemes of the measuring points were provided according to three different search sequences: gradual deletion, direct acquisition, and gradual accumulation, as indicated in Table 2.

Table 2. Sensor placement using three methods.

Searching Sequence	EI	MKE	EI-MKE
Gradually deleted	1X 2Z 6X 7Z 11Z 13Z	2Z 5Z 7Z 9Z 13Z 15Z	2X 2Z 4Z 7X 7Z 13Z
Direct acquisition	2Z 7Z 11Z 13Z 9Z 15Z	2Z 5Z 7Z 9Z 13Z 15Z	2Z 7Z 13Z 9Z 15Z 5Z
Gradually accumulated	2Z 9Z 10Z 3Z 11Z 4Z	2Z 5Z 7Z 9Z 13Z 15Z	2Z 9Z 10Z 3Z 7Z 15Z

Four evaluation criteria were used to evaluate the layout of the measuring points, as shown in Figure 3. In order to avoid confusion, the maximum MAC of the off-diagonal element of the autocorrelation matrix of the measuring point is MAC_n. MAC_n characterizes the linear independence of the measuring point mode. The smaller the MAC_n, the better the orthogonality of the test mode and the better the anti-noise ability of the measuring point. The minimum diagonal element of the correlation matrix formed by the extended complete mode and the structural theoretical mode is MAC_d. MAC_d represents the correlation between the complete mode formed by the expansion of the measuring point and the complete mode information of the structure. The larger the MAC_d, the higher the correlation between the extended mode and the theoretical mode and the more complete the extended structural information.

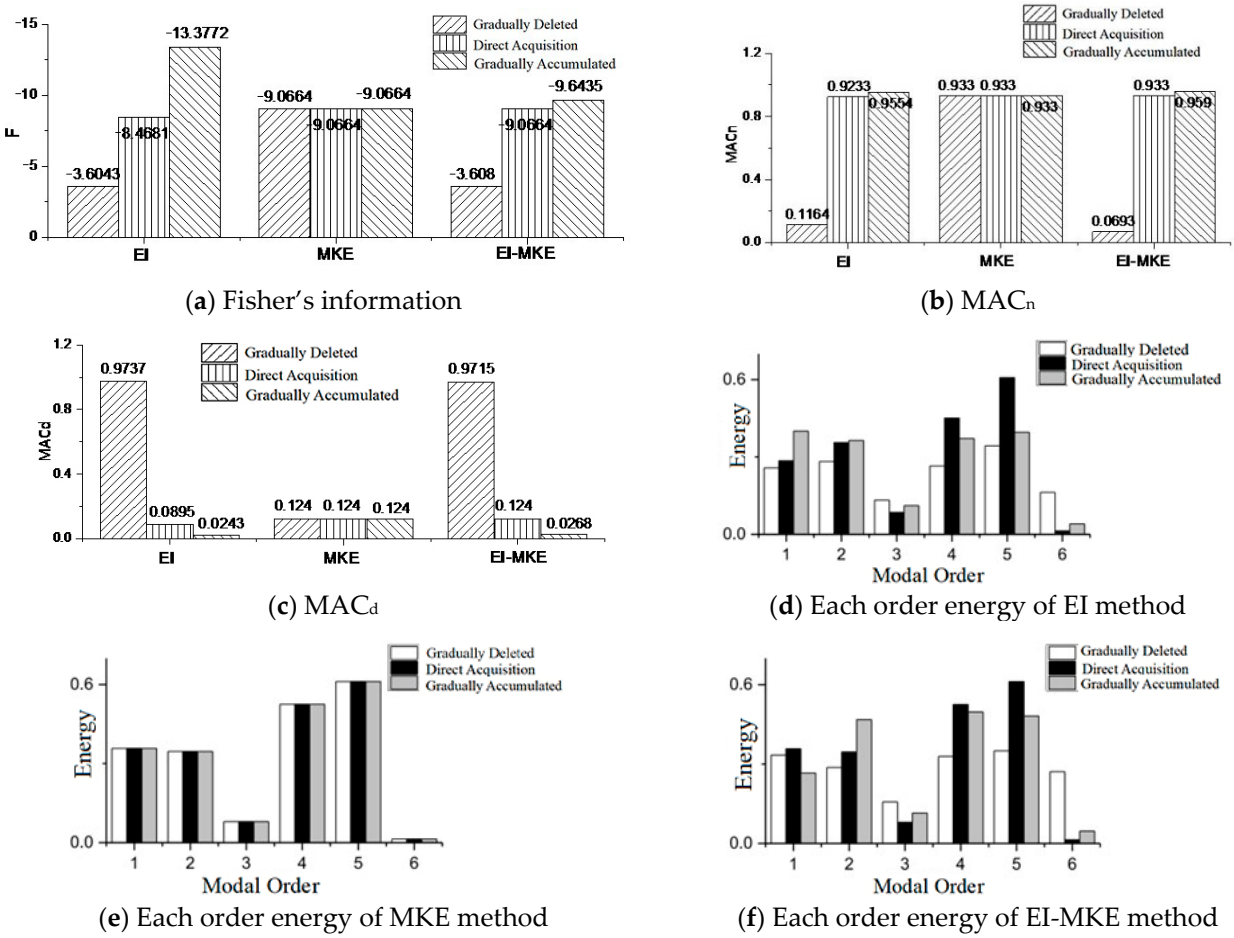

(**a**) Fisher's information (**b**) MAC_n

(**c**) MAC_d (**d**) Each order energy of EI method

(**e**) Each order energy of MKE method (**f**) Each order energy of EI-MKE method

Figure 3. Sensor placement evaluation.

From the above results, the search order had no effect on the MKE method, and the results of the three search orders were the same. The search order had a great influence on the EI method and the EI-MKE method; as shown in Figure 3a, the obtained measurement points were gradually deleted, and the maximum Fisher information value was obtained; as shown in Figure 3b, the measured point modes obtained by gradually deleting had good orthogonality; and as shown in Figure 3c, after gradually deleting the obtained measuring points for complete modal expansion, the structural expansion mode had the greatest correlation with the theoretical mode. Therefore, the following algorithms in this paper were all based on the arrangement of the measuring points obtained by the gradual deletion process.

It can be seen from the results of the energy map shown in Figure 3d–f that the gradual deletion process, compared with the direct acquisition and gradual accumulation processes, obtained relatively less energy at the measuring point. However, it can be seen from the modal expansion results that as long as the vibration mode of the measuring point could be obtained, this lower energy did not affect the expansion of the incomplete mode of the structure into a complete mode. Therefore, the subsequent evaluation of the measuring point arrangement in this paper no longer considered the modal energy problem of the measuring points.

2.4. Algorithm Optimization

The three measuring point arrangement methods of the above plane truss example were evaluated, and the following conclusions were drawn:

(1) From the perspective of Fisher's determinant, the information of the measuring point arrangement obtained by the EI method was slightly higher than that obtained by

the EI-MKE method, and the Fisher information obtained by the MKE algorithm was the least.

(2) From the perspective of MAC_n, the modal orthogonality of the measuring points obtained by the EI-MKE method was the best, followed by the EI method. The arrangement of the measuring points obtained by the MKE method and the non-diagonal elements of the MAC matrix reached more than 0.9, indicating that the orthogonality of the test mode was poor and that there was a cross mode.

(3) From the perspective of MAC_d, the extended mode obtained by the EI method had the best correlation with the theoretical mode of the structure, followed by the EI-MKE method. The minimum value of the extended mode MAC_d of the measuring point obtained by the MKE method reached within 0.2, indicating that the extended mode was almost orthogonal to the theoretical mode of the order and that the expansion result was poor.

Based on the above information, the MKE method was used to obtain the structural modal measurement points. Compared with the EI method and the EI-MKE method, there is a large lack of modal information, which is not suitable for the spatial grid structures when arranging the measurement points. The EI method and the EI-MKE method have their own advantages, so the application dimension of the algorithm should be expanded.

The structural dimension was expanded to three dimensions, and a 3×7 square pyramid grid structure model was established, as shown in Figure 4. The grid length was set as 1.5 m, the grid thickness was set as 1.2 m, and a fixed hinge support was set on the opposite side of the lower chord. The elastic modulus of the rod was set as 2.06×10^{11} N/m^2, the cross-sectional area of the upper and lower chords was set as 1.07×10^{-3} m^2, the cross-sectional area of the web member was set as 9.04×10^{-4} m^2, the material density of the rod was set as 7.85×10^3 Kg/m^3, and the added mass was set as 1700 Kg. The first six theoretical frequencies and modes of the structure were obtained by modal analysis, as shown in Figure 5.

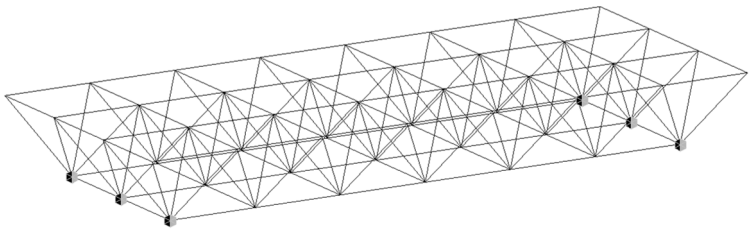

Figure 4. Midas Gen grid structure model.

Two algorithms (EI and EI-MKE) were applied. The first six modes and six measuring points were the targets. The node numbers of the grid structure are shown in Figure 6, and the arrangement results of the measuring points are shown in Table 3. Fisher's information, MAC_n, and MAC_d were used to evaluate the results of the measuring point arrangement, as shown in Figure 7.

Table 3. Sensor placement using EI and EI-MKE methods.

Measuring Point Arrangement Method	Measuring Point
EI	13Y 16Y 25Z 28Z 49Z 52Z
EI-MKE	21Y 25Z 28Z 49Z 50Z 52Z

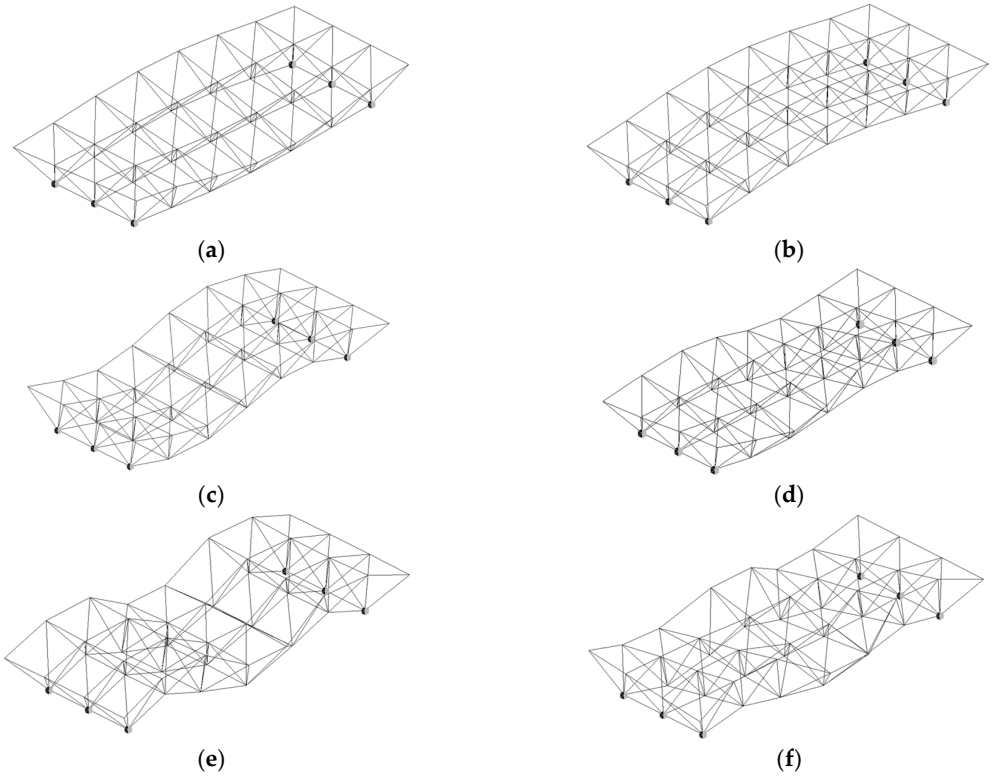

Figure 5. The theoretical frequencies and vibration modes for the first six modes of the grid structure. (**a**) First mode of vibration (4.713 Hz); (**b**) Second mode of vibration (5.100 Hz); (**c**) Third mode of vibration (5.524 Hz); (**d**) Fourth mode of vibration (9.290 Hz); (**e**) Fifth mode of vibration (10.741 Hz); (**f**) Sixth mode of vibration (12.953 Hz).

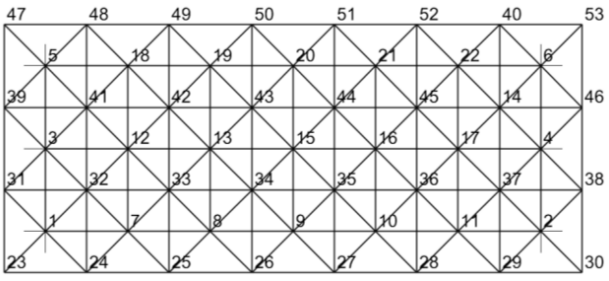

Figure 6. Node numbers of 3 × 7 grid structure.

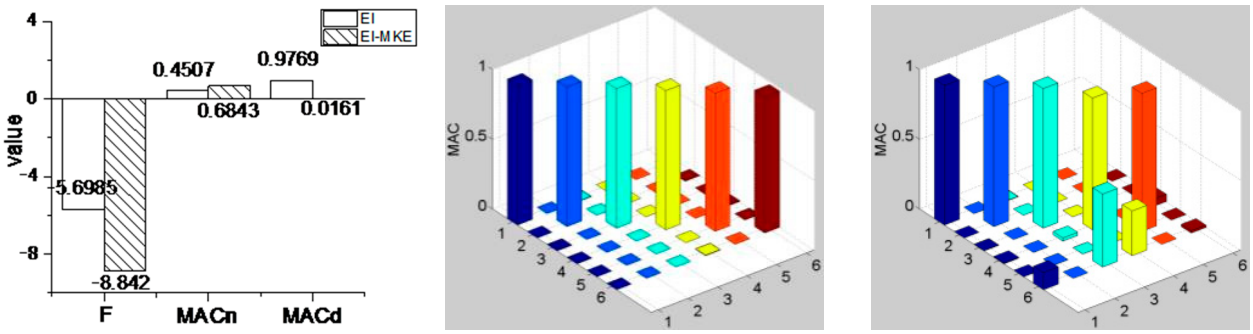

(**a**) (**b**) (**c**)

Figure 7. Sensor placement evaluation. (**a**) Evaluating indicator; (**b**) MAC of extended mode of EI method; (**c**) MAC of extended mode of EI-MKE method.

As shown in Figure 7, the extended mode MAC_d value was derived from the extended sixth-order mode. Although the EI-MKE method had good expansion results for the first five modes, the sixth-order MAC_d value was very small and almost orthogonal to the sixth-order theoretical mode, indicating that the EI-MKE method lost the sixth-order mode during the expansion process. The EI method was better than the EI-MKE method in terms of the amount of information at the measuring point, the orthogonality of the measuring point, and the integrity of the extended mode. Therefore, for a three-dimensional spatial grid structures, the EI method can obtain more measuring point arrangement information, which is more suitable for the measuring point arrangement of the spatial grid structures. The MAC matrix of the modal components in the three directions of the extended mode of the structure is the output, as shown in Figure 8.

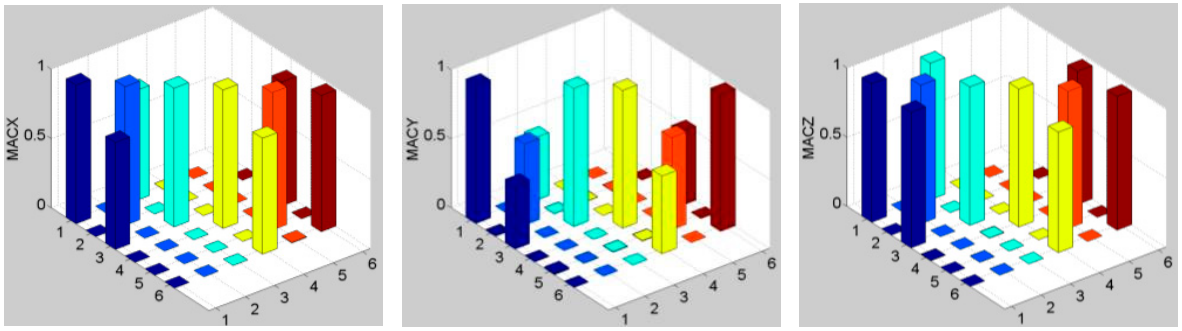

(**a**) (**b**) (**c**)

Figure 8. Mode expansion verification. (**a**) MACX; (**b**) MACY; (**c**) MACZ.

3. Arrangement of Structural Measuring Points with Damage

In order to verify whether the damaged structure still has a high correlation with the theoretical vibration mode of the original structure, this section performs a numerical simulation on the above grid example so that the number of structural members varies from zero damage to half damage, and the structural frequency and vibration mode are calculated. At the same time, the structural vibration mode and the MAC value of the original structure are calculated. Since the number of structural members in the example is 168, when the damage of the members reaches half, there may be too many damage combinations. For this reason, the concept of member sensitivity was introduced, and the single member damage was assumed to calculate the structural sensitivity coefficient. Then, in order to obtain the randomness of the structural vibration mode, random damage values of 0–10%, 20–30%, and 40–50% were imposed on the structural members. In the case of progressive damage of the rod, the MAC matrix of the first six orders of the damaged structure vibration mode and the theoretical vibration mode was calculated successively, and the MAC was counted as shown in Table 4.

Table 4. Damaged structure information statistics under different vibration mode member sensitivities.

Damage Situation	No.	Min(f)	Δf	MAC					
				>0.99	0.95–0.99	0.90–0.95	0.1–0.9	0.05–0.1	<0.05
0–10%	1	6.358	4.61%	168	0	0	0	0	0
	2	6.868	4.78%	168	0	0	0	0	0
	3	7.421	5.01%	168	0	0	0	0	0
	4	12.475	5.04%	168	0	0	0	0	0
	5	14.445	4.90%	168	0	0	0	0	0
	6	17.356	5.13%	168	0	0	0	0	0
20–30%	1	5.594	16.08%	115	50	3	0	0	0
	2	6.050	16.12%	67	101	0	0	0	0
	3	6.537	16.32%	77	63	26	2	0	0
	4	11.028	16.06%	154	14	0	0	0	0
	5	12.820	15.60%	115	53	0	0	0	0
	6	15.357	16.05%	152	16	0	0	0	0
40–50%	1	4.742	28.86%	63	55	17	33	0	0
	2	5.132	28.84%	17	28	66	48	1	8
	3	5.565	28.76%	72	12	21	63	0	0
	4	9.456	28.03%	68	100	0	0	0	0
	5	10.794	28.94%	26	78	54	10	0	0
	6	13.006	28.91%	27	119	22	0	0	0

For this space truss, as shown in Table 4, there was a positive correlation between the decrease in the structural frequency and the level of correlation of the structural vibration modes. In the range of a 5% decrease in the frequency, the structural vibration mode was highly consistent with the theoretical vibration mode. With the increase in the damage degree, such as with a decrease in frequency to about 28%, the vibration mode of each order of the grid structure deviated from the theoretical vibration mode of the undamaged structure to varying degrees, especially the third-order vibration mode, and the occurrence of MAC values below 0.9 happened 37.5% of the time.

The measurement point arrangement of the grid structure under undamaged and damaged conditions was carried out. The node number is shown in Figure 6, and the arrangement of the measuring points by the EI method is shown in Table 5. The theoretical distribution of the measuring points was the union distribution of 168 kinds of measuring points, which was obtained according to the damage order. MAC_n comes from the MAC matrix of the modal orthogonality check of the measuring points obtained by the non-destructive structural measuring points and the actual structural vibration mode displacement, which is the most unfavorable description in all the measuring points. MAC_d is derived from the MAC matrix of the extended modal correlation check of the measurement point arrangement corresponding to MAC_n.

It can be seen from Table 5 that after the occurrence of damage to the structure, the theoretical distribution of the measuring points changed, and as the damage increased, the orthogonality of the structural test mode became worse and worse, and the extended mode also showed a worse and worse correlation. However, the MAC values that characterized the modal orthogonality and the extended modal correlation of the measuring points were not much different from those of the undamaged structure. The number of combined measuring points could reflect the demand for measuring points of the first to sixth modes of the undamaged structures and damaged structures. In the case of damage within 10%, the number of merged elements was 18. With the increase in the damage degree, the number of merged measuring points changed to 20. According to the distribution of the measuring points generated by random damage, the change in the merging set was not large and basically remained stable. This shows that these degrees of freedom had the highest sensitivity to the first to sixth modes of the structure, and the structure had a basically stable distribution of measuring points. While the structural members

were damaged and the vibration modes changed, the possibility of the measuring point distribution covering all the possible vibration modes could be basically guaranteed.

Table 5. Sensor placement information under different levels of damage.

Damage Quantity	No.	Theoretical Distribution of Measuring Points	MAC_n	MAC_d
0		13Y 16Y 25Z 28Z 49Z 52Z	0.4507	0.9769
0–10%	1	13Y 16Y 25Z 26Y 26Z 27Y 27Z 28Z 49Y 49Z 50Z 51Y 51Z 52Y 52Z	0.4552	0.9734
	2	13Y 16Y 25Z 26Y 26Z 27Y 27Z 28Y 28Z 49Y 49Z 50Y 50Z 51Z 52Z	0.4552	0.9749
	3	13Y 16Y 25Y 25Z 26Y 26Z 27Y 27Z 28Z 49Y 49Z 50Z 51Y 51Z 52Y 52Z	0.4547	0.9728
	4	13Y 16Y 25Y 25Z 26Y 26Z 27Y 27Z 28Y 28Z 49Y 49Z 50Y 50Z 51Y 51Z 52Y 52Z	0.4556	0.9740
	5	13Y 16Y 25Y 25Z 26Y 26Z 27Y 27Z 28Y 28Z 49Z 50Z 51Z 52Y 52Z	0.4574	0.9716
	6	13Y 16Y 25Z 26Y 26Z 27Y 27Z 28Y 28Z 49Y 49Z 50Y 50Z 51Y 51Z 52Y 52Z	0.4568	0.9729
Merge measuring points		13Y 16Y 25Y 25Z 26Y 26Z 27Y 27Z 28Y 28Z 49Y 49Z 50Y 50Z 51Y 51Z 52Y 52Z		
20–30%	1	10Y 13Y 16Y 25Y 25Z 26Z 27Y 27Z 28Y 28Z 49Y 49Z 50Y 50Z 51Y 51Z 52Z	0.4643	0.9646
	2	10Y 13Y 16Y 25Z 26Y 26Z 27Y 27Z 28Y 28Z 49Y 49Z 50Y 50Z 51Y 51Z 52Y 52Z	0.4652	0.9621
	3	10Y 13Y 16Y 25Y 25Z 26Y 26Z 27Y 27Z 28Y 28Z 49Y 49Z 50Y 50Z 51Y 51Z 52Y 52Z	0.4646	0.9640
	4	8Y 13Y 16Y 25Y 25Z 26Y 26Z 27Y 27Z 28Y 28Z 49Y 49Z 50Y 50Z 51Y 51Z 52Y 52Z	0.4648	0.9634
	5	8Y 13Y 16Y 25Y 25Z 26Y 26Z 27Y 27Z 28Y 28Z 49Y 49Z 50Y 50Z 51Z 52Y 52Z	0.4806	0.9389
	6	8Y 13Y 16Y 25Y 25Z 26Y 26Z 27Y 27Z 28Y 28Z 49Y 49Z 50Y 50Z 51Z 52Y 52Z	0.4694	0.9590
Merge measuring points		8Y 10Y 13Y 16Y 25Y 25Z 26Y 26Z 27Y 27Z 28Y 28Z 49Y 49Z 50Y 50Z 51Y 51Z 52Y 52Z		
40–50%	1	8Y 10Y 13Y 16Y 25Y 25Z 26Z 27Y 27Z 28Y 28Z 49Y 49Z 50Y 50Z 51Y 51Z 52Z	0.4689	0.9467
	2	10Y 13Y 16Y 25Z 26Y 26Z 27Y 27Z 28Y 28Z 49Y 49Z 50Z 51Y 51Z 52Z	0.4769	0.9448
	3	8Y 10Y 13Y 16Y 25Z 26Y 26Z 27Z 28Y 28Z 49Y 49Z 50Z 51Y 51Z 52Z	0.4688	0.9678
	4	8Y 10Y 13Y 16Y 25Y 25Z 26Y 26Z 27Z 28Y 28Z 49Y 49Z 50Y 50Z 51Z 52Z	0.4731	0.9124
	5	8Y 10Y 13Y 16Y 25Z 26Y 26Z 27Y 27Z 28Y 8Z 49Y 49Z 50Y 50Z 51Z 52Y 52Z	0.5114	0.8482
	6	8Y 10Y 13Y 16Y 25Y 25Z 26Y 26Z 27Y 27Z 28Y 28Z 49Y 49Z 50Z 51Z 52Y 52Z	0.4804	0.9345
Merge measuring points		8Y 10Y 13Y 16Y 25Y 25Z 26Y 26Z 27Y 27Z 28Y 28Z 49Y 49Z 50Y 50Z 51Y 51Z 52Y 52Z		

4. Study on the Number of Measuring Points

In order to ensure the spatial orthogonality of the test modes, many scholars use MAC_n to achieve a stable value as the upper limit of the number of measuring points, which lacks scientific basis. The modal expansion of the structure was carried out by using the three-stage improved Guyan recursive technique. It can be seen from Table 4 that within 10% damage, the real vibration mode of the structure had a good correlation with

the theoretical vibration mode, and the MAC reached more than 0.99. Therefore, for the above grid example, the first six modes were the target modes, and the structural expansion mode was related to the theoretical vibration mode. The MAC reached 0.99 as the goal, and the change in the number of measuring points was studied compared with MAC_n, as shown in Figure 9.

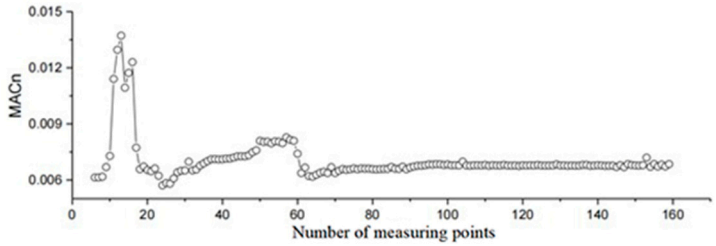

(**a**) MACn

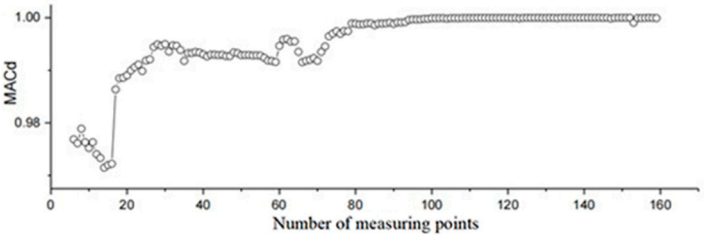

(**b**) MACd

Figure 9. Parameter change with increase in sensor number.

The orthogonality of the test modes is intended to prevent the crossing of the test modes, and if the modes of the measurement points are crossed, they can be tested. The arrangement of these points should aim to obtain as much structural information as possible; thus, MAC_d is considered superior to MAC_n as a numerical target. For this example, as shown in Figure 9, a minimum MAC_n value was reached when the number of measuring points reached 24; however, more than 60 measuring points were needed for the measuring point arrangement to achieve a stable state. Yet, when the number of measuring points was 24, the MAC_n value was found to be smaller than that of the sufficient number of measuring points until a stable and low MAC_n value was reached. Therefore, when the MAC_n value is taken as the condition, it is deemed the most economical and reasonable to select 24 measuring points. For MAC_d, when the number of measurement points reached 21, the correlation between the measured vibration mode and the theoretical vibration mode was greater than 0.99. Furthermore, the MAC_d value at 21 measurement points differed the least from the MAC_d value when the number of measurement points was sufficiently high for the MAC_d value to stabilize. Therefore, it is considered the most economically reasonable to use 21 measurement points when the MAC_d value is the criterion. From the perspective of the number of measurement points, the number of measurement points obtained with MAC_d as the target was found to be smaller than that with MAC_n as the target.

5. Conclusions

In this paper, through the verification of plane truss and grid structure examples, the problem of measuring point arrangement was studied. The main conclusions are as follows:

(1) The EI method, MKE method, and EI-MKE method, which have a great influence on the arrangement of the measuring points, were compared and analyzed. When the three methods were applied to the grid structure, the measuring points obtained by the gradually deleted search process had the greatest correlation between the structural extended mode and the theoretical mode. At the same time, it was concluded that the

EI method is the most suitable method for the arrangement of the measuring points in spatial grid structures.

(2) The effect of the search order on the MKE method was negligible, and the results for the three search orders were identical. However, the search order greatly influenced the EI method and the EI-MKE method. The MKE method was found to have significant missing modal information compared to the EI method and the EI-MKE method, making it unsuitable for measuring point layout in spatial grid structures. Both the EI method and the EI-MKE method have their own advantages. With reference to the extended MAC_d value of the sixth-order mode derived from the extended mode, it was observed that although the EI-MKE method yielded good expansion results for the first five order modes, the sixth-order MAC_d value was very small and was almost orthogonal to the sixth-order theoretical mode, indicating that the sixth-order mode is lost in the expansion process of the EI-MKE method. The EI method was found to be superior to the EI-MKE method in terms of measuring point information, measuring point orthogonality, and extended mode integrity. Therefore, the EI method can obtain more measuring point arrangement information for three-dimensional spatial grid structures and is considered more suitable for determining the measuring point arrangement of spatial grid structures.

(3) The numerical analysis of the grid was carried out, and the most unfavorable situation of structural damage was determined by the sensitivity method. The correlation of the structural modes under various damage conditions was compared. The statistical information shows that the structural frequency of the structure had a large loss under the different damage degrees, and the structural vibration mode and the vibration mode of the undamaged structure still maintained a good correlation. In particular, when the structural frequency decrease was less than 5%, the low-order vibration modes of the structure were still highly consistent with the theoretical vibration modes of the undamaged structure.

(4) It was found that with the increase in the damage amount, the MAC values of the modal orthogonality and extended modal correlation of the measuring points were less different from those of the undamaged structures. This shows that the structure had a basically stable distribution of measuring points that could basically cover the possibility of the measuring point distribution of all possible vibration modes.

(5) Combined with the three-level improved Guyan recursive technique, in order to obtain better complete modal parameters, the demand for the number of measuring points was studied, and it was concluded that the number target of MAC_d is better than that of MAC_n.

Author Contributions: Collection of data, Writing—Original Data, Methodology, C.Z.; Design of the study, Investigation, J.W.; Project administration, Writing—Review & Editing, G.S.; Writing—Review & Editing, Visualization, J.H.; Analyzed the data, Validation, Q.X.; Writing—Original Draft, Y.L.; Funding acquisition, Supervision, M.L. All authors have read and agreed to the published version of the manuscript.

Funding: The research was funded by the Key Research and Development Projects of Shanxi Province [2022LL-JB-13].

Data Availability Statement: The original contributions presented in the study are included in the article. For further inquiries, please contact the corresponding author.

Conflicts of Interest: Author Chunjuan Zhou and Mingliang Liu are employed by the Shaanxi Architecture Science Research Institute Co., Ltd. The remaining authors declare that the research was conducted in the absence of any commercial or financial relationships that could be construed as a potential conflict of interest.

References

1. Basu, B.; Bursi, O.S.; Casciati, F.; Casciati, S.; Del Grosso, A.E.; Domaneschi, M.; Faravelli, L.; Holnicki-Szulc, J.; Irschik, H.; Krommer, M.; et al. A European Association for the Control of Structures joint perspective. Recent studies in civil structural control across Europe. *Struct. Control Health Monit.* **2014**, *21*, 1414–1436. [CrossRef]
2. Chen, Y. Advances and prospects for optimal sensor placement of structural health monitoring. *J. Vib. Shock* **2015**, *45*, 1–9+52.
3. Yang, C.; Zheng, W.; Zhang, X. Optimal sensor placement for spatial lattice structure based on three-dimensional redundancy elimination model. *Appl. Math. Model.* **2018**, *66*, 576–591. [CrossRef]
4. Xiao, F.; Hulsey, J.L.; Balasubramanian, R. Fiber optic health monitoring and temperature behavior of bridge in cold region. *Struct. Control Health Monit.* **2017**, *24*, e2020. [CrossRef]
5. Xiao, F.; Hulsey, J.L.; Chen, G.S.; Xiang, Y. Optimal static strain sensor placement for truss bridges. *Int. J. Distrib. Sens. Netw.* **2017**, *13*, 1550147717707929. [CrossRef]
6. Kammer, D.C. Sensor placement for on orbit modal identification and correlation of large space structures. *J. Guid. Control Dyn.* **1991**, *14*, 251–259. [CrossRef]
7. Lim, T.W. Actuator/sensor placement for modal parameter identification of flexible structures. *Modal Anal. Int. J. Anal. Exp. Modal Anal.* **1993**, *8*, 1–13.
8. Wu, D.; Wu, Z.; Qin, X.; Yang, H. Optimal sensor placement based on two-step effective configuration method. *J. Xihua Univ. Nat. Sci.* **2008**, *27*, 48–51.
9. Hua, B. Study on sensor layout and damage identification of building cover in high speed railway station. *Build. Sci.* **2021**, *37*, 28–36.
10. Mei, H.; Lin, X. Damage Orientation Method Based on the Modal Kinetic Energy. *Appl. Mech. Mater.* **2012**, *256–259*, 1112–1116.
11. Gomes, G.F.; de Almeida, F.A.; da Silva Lopes Alexandrino, P.; da Cunha, S.S.; de Sousa, B.S.; Ancelotti, A.C. A multiobjective sensor placement optimization for SHM systems considering Fisher information matrix and mode shape interpolation. *Eng. Comput.* **2019**, *35*, 519–535. [CrossRef]
12. Liu, W.; Gao, W.; Liu, H. Theoretical Research on Two Improved Optimal Sensor Placement Methods. *Appl. Mech. Mater.* **2013**, *2544*, 1122–1129. [CrossRef]
13. Li, D.; Zhang, Y.; Ren, L.; Li, H. Sensor placement method and evaluation criteria in structural health monitoring. *Adv. Mech.* **2011**, *41*, 39–50.
14. Zhang, B.-Y.; Ni, Y.-Q. A data-driven sensor placement strategy for reconstruction of mode shapes by using recurrent Gaussian process regression. *Eng. Struct.* **2023**, *284*, 115998. [CrossRef]
15. Zhan, Z.; Fang, B.; Wan, S.; Bai, Y.; Hong, J.; Li, X. Application of a hybrid-driven framework based on sensor optimization placement for the thermal error prediction of the spindle-bearing system. *Precis. Eng.* **2024**, *89*, 174–189. [CrossRef]
16. Xu, Z.; Wang, S.; Zhang, X.L.; He, G. Optimal sensor placement for ensemble-based data assimilation using gradient-weighted class activation mapping. *J. Comput. Phys.* **2024**, *514*, 113224. [CrossRef]
17. Guo, X.; Zhang, J.; Zeng, Q.; Zhu, S.; Zong, S. Performance-based optimal sensor placement method for single-layer reticulated shells considering modal observability and damage identifiability. *Thin-Walled Struct.* **2023**, *188*, 110809. [CrossRef]
18. Xin, J.; Jiang, Y.; Wu, B.; Yang, S.X. Intelligent Bridge Health Monitoring and Assessment. *Buildings* **2023**, *13*, 1834. [CrossRef]
19. Deng, Z.; Huang, M.; Wan, N.; Zhang, J. The Current Development of Structural Health Monitoring for Bridges: A Review. *Buildings* **2023**, *13*, 1360. [CrossRef]
20. Sun, X.; Ou, J. Optimal sensor placement based on sensitivity of damage parameters. *J. Harbin Inst. Technol.* **2010**, *42*, 1530–1535.
21. Lin, J.; Xu, Y.; Zhan, S. Experimental investigation on multi-objective multi-type sensor optimal placement for structural damage detection. *Struct. Health Monit.* **2019**, *18*, 882–901. [CrossRef]
22. Cha, Y.J.; Agrawal, A.K.; Kim, Y.; Raich, A.M. Multi-objective genetic algorithms for cost-effective distributions of actuators and sensors in large structures. *Expert Syst. Appl.* **2012**, *39*, 7822–7833. [CrossRef]
23. Chang, M.; Pakzad, N.S. Optimal Sensor Placement for Modal Identification of Bridge Systems Considering Number of Sensing Nodes. *J. Bridge Eng.* **2014**, *19*, 04014019. [CrossRef]
24. Xiao, F.; Sun, H.; Mao, Y.; Chen, G.S. Damage identification of large-scale space truss structures based on stiffness separation method. In *Structures*; Elsevier: Amsterdam, The Netherlands, 2023; Volume 53.
25. Xiao, F.; Zhu, W.; Meng, X.; Chen, G.S. Parameter identification of frame structures by considering shear deformation. *Int. J. Distrib. Sens. Netw.* **2023**, *2023*, 6631716. [CrossRef]
26. Liu, F.; Guo, P.; Wang, C.; Dong, S. A direct mode shape expansion method. *Eng. Mech.* **2012**, *29*, 28–32.
27. Brincker, R.; Skafte, A.; López-Aenlle, M.; Sestieri, A.; D'Ambrogio, W.; Canteli, A. A local correspondence principle for mode shapes in structural dynamics. *Mech. Syst. Signal Process.* **2014**, *45*, 91–104. [CrossRef]
28. Zhao, J.; Zhang, L.; Xiang, B.; Wan, Y. A structural damage identification method under incomplete test data. *Chin. J. Appl. Mech.* **2010**, *27*, 670–673+845–846.
29. Mousavi, M.; Gandomi, H.A. A hybrid damage detection method using dynamic-reduction transformation matrix and modal force error. *Eng. Struct.* **2016**, *111*, 425–434. [CrossRef]
30. Yang, J.; Dong, C. Structural damage identification method based on incomplete modal information. *Chin. J. Comput. Mech.* **2019**, *36*, 290–296.

31. Civalek, Ö.; Öztürk, B.; Yavaş, A. Nonlinear transient dynamic response of clamped rectangular plates on two-parameter foundations by the algorithm of the singular convolution. *Int. J. Sci. Technol.* **2007**, *2*, 165–177.
32. Liu, B.; Yao, Y.; Ye, G. Study of optimal sensor placement for cable-stayed bridge. *Eng. Mech.* **2005**, *22*, 171–176.
33. Liu, G.; Yang, B.; Liu, Y.; Wong, S. Comparative analysis of three sensor placement optimization algorithms in tied arch bridge. *J. Vib. Shock* **2008**, *27*, 190–193.
34. Li, D.S.; Li, H.N.; Fritzen, C.P. The connection between effective independence and modal kinetic energy methods for sensor placement. *J. Sound Vib.* **2007**, *305*, 945–955. [CrossRef]
35. Zhan, J.Z.; Yu, L. An Effective Independence-Improved Modal Strain Energy Method for Optimal Sensor Placement of Bridge Structures. *Appl. Mech. Mater.* **2014**, *670*, 1252–1255. [CrossRef]
36. Desforges, M.J.; Cooper, J.E.; Wright, J.R. Mode tracking during flutter testing using the modal assurance criterion. *Proc. Inst. Mech. Eng. Part G: J. Aerosp. Eng.* **1996**, *210*, 27–37. [CrossRef]
37. Kuljus, K.; von Rosen, D. Rank covariance matrix estimation of a partially known covariance matrix. *J. Stat. Plan. Inference* **2008**, *138*, 3667–3673. [CrossRef]
38. Cui, W.; Zhang, X.; Liu, Y. Covariance matrix estimation from linearly-correlated Gaussian samples. *IEEE Trans. Signal Process.* **2019**, *67*, 2187–2195. [CrossRef]
39. Kim, S.H.; Cho, C. Effective independence in optimal sensor placement associated with general Fisher information involving full error covariance matrix. *Mech. Syst. Signal Process.* **2024**, *212*, 111263. [CrossRef]